International Journal of Applied Engineering Research ISSN 0973-4562 Volume 13, Number 15 (2018) pp. 12244-12258

The Adhesion Component of Shear Strength in Basalt Fiber Reinforced Plastics based on Epoxy Binders

Orlov M.A.,
Head of Laboratory, IEC CM Bauman MSTU, Russia.

Kalinnikov A.N.,
Head of Laboratory, IEC CM Bauman MSTU, Russia.

Tereshkov A.G.,
Leading engineer-designer, IEC CM Bauman MSTU, Russia.

Shlykova A.N.,
Project Manager, "Kamenny vek" LLC

Abstract

The practical studies on the contribution of the adhesion component to the shear strength in composite samples based on basalt fiber and epoxy matrices are presented in the article. Studies were conducted to identify the optimal combination of binders and lubricants for the development of industrial technological solutions and manufacturing structural composite products with enhanced performance characteristics.

The article presents the results of testing the actual sample sets, analysis of the effectiveness of research methods used in evaluating adhesive strength, their compatibility, and final conclusions.

Keywords: basalt plastics, basalt fiber, composite materials, technology, structural products, polymer binders, lubricants.

INTRODUCTION

The work presented in this article was performed within research and engineering facilities of "Composites of Russia" Technological Center, Bauman Moscow State Technical University, under creation of a full technological cycle for industrial production of structural composite products based on national samples of basalt fibers, polymer binders and effective lubricants.

The following tasks should be completed in the course of the study:

1) Rationale for choosing research methods to evaluate the adhesion strength of basalt plastic samples manufactured under various combinations of polymer binders, lubricants, structure and geometry of implementation.

2) Research (evaluation) of the adhesion component of shear strength in the experimental set of samples formed upon the combination of the binder type and the lubricant, using diverse test methods.

3) Assessment of applicability and technological constraints of test methods used in this research.

Presented studies were funded by the Ministry of Education of the Russian Federation via Contracts No 03.G25.31.0264 and RFMEFI57417X0160.

MATERIALS AND METHODS

Standard methods used to evaluate the adhesive strength of compounds include shear, separation, and torsion of contacting bodies relative to each other. Tests for evaluating the adhesive strength of compounds were performed by different methods on bodies of various shapes and manufactured of different materials. The test results indicate that the strength of compounds is affected by numerous parameters (surface microroughness, heat treatment, test temperature, sample geometry, etc.). The existing methods can be classified into micro- and macromechanical.

Several micromechanical methods are currently used to determine the strength of adhesive bonding between polymers and the fiber surface. In most cases, the measured parameter is the force required to tear a single fiber out of a block, drop or film (Fig. 1) [1]. The adhesion strength τ is thus calculated by the equation:

$$\tau = \frac{F}{\pi d l},$$

where F is the pulling force, d is the fiber diameter, l is the contact length.

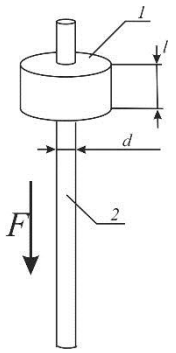

Figure 1. The fiber tear-out from the matrix layer, schematic view of the method. 1 – matrix, 2 – fiber.

Another variant implies extending the matrix with a thin encapsulated fiber in it [2]. Here, the measured parameter is the average length *l* of resulting fiber fragments, which is correlated with the adhesion strength by the Kelly's ratio:

$$\tau = C \times \frac{\overline{\delta_l} \times d}{2 \times l},$$

where $\overline{\delta_l}$ is the strength of a fibre of length *l*, C is a correlating multiplier [2].

It should be noted that the τ value, despite being called the adhesive strength, characterizes adhesion only indirectly. The adhesive strength measured in the experiments reflects both the nature of physico-chemical interactions at the interface, and deformation properties of the system components. The combination of these factors depends considerably on the sample geometry, the stress field in it and characterizes bonding of this pair, rather than the pair as such [1]. For this reason, a comparison of test results for the same polymer-fiber system obtained by different researchers reveals a large data scatter.

The local adhesive strength τ_a was suggested in [3] as a parameter characterizing the strength of the adhesive bond more correctly. It represents the voltage required to produce a shear at a given point of the interface. The difference between τ and τ_a is illustrated in Figs. 2 and 3, which show the stress distribution along the fiber when pulled out of a polymer droplet.

This distribution is essentially heterogeneous in actual samples. First, when an external load is applied to the elastic fiber, the maximum shear stress develops at the point of its entry into the matrix. Second, due to the differing coefficients of thermal expansion in the fiber and the matrix, thermal stresses emerge at the interface, which are symmetrically distributed along the contact length. The actual distribution of shear stress in a sample represents a superposition of elastic and thermal stresses. The elastic stresses increase along with the increase in external load, thus, the resulting curve is shifted upward on the ordinate axis. At certain time moment, the local force at the fiber entry point into the matrix becomes large enough to cause the break of adhesion bond at that point. This force is indicated as τ_a and is used to generate adequately strict values characterizing the strength of adhesive bond. In calculating the adhesive strength, the shear force applies to the entire contact length; hence, the value of τ represents a certain average value. Actually, τ values can be far smaller than τ_a, as evidenced by a number of experimental studies.

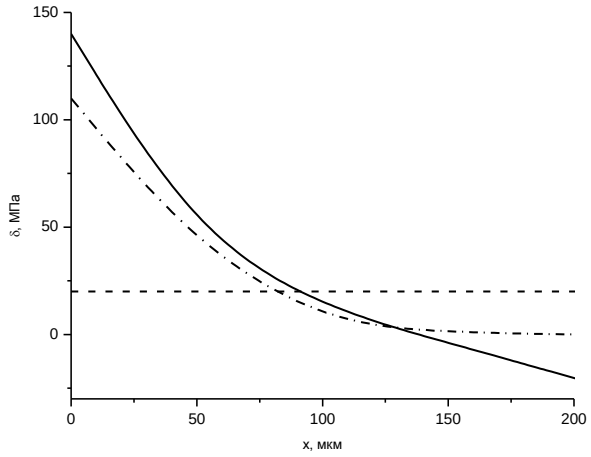

Figure 2. Typical instantaneous distribution of shear stresses at the fiber-matrix interface. (---) – average adhesive strength; (-.-) – elastic shear stress; (-) – total shear stress.

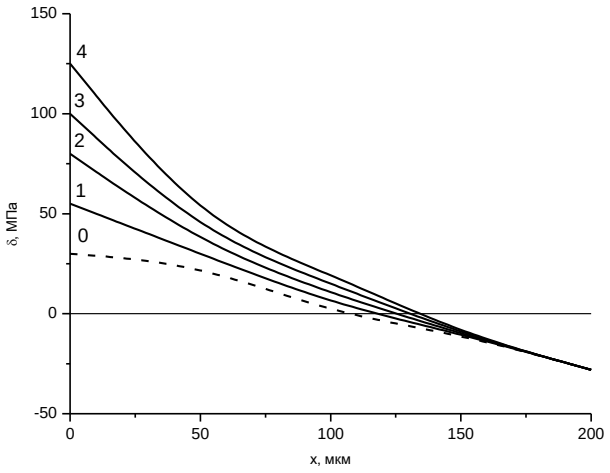

Figure 3. Increase in interfacial shear stresses with increasing external load applied to the fiber. 0 –residual thermal stress; 1-4 – total shear stress at rising load; x – coordinate by the fiber length.

Calculations of τ_a values in practice imply, as a rule, extrapolation of the dependence of the measured adhesive strength on the contact length onto the zero value of this length. Unlike the τ value, the local adhesive strength reflects the intensity of physico-chemical interaction at the interface, i.e., represents a quantitative characteristic of the adhesion *proper* and does not depend on the sample geometry, as well as on residual stresses and the deformation term. Methods relying on the fiber tear-out from the polymer layer demonstrate a very high convergence between several series of experiments [4]. This is achieved by testing a sufficiently large number of micro samples (at least, 60) to build one point of the plot.

It should be noted that micromethods provide a comparative representation of the adhesive interaction between the fiber and the matrix, and are acceptable for comparative tests. At the same time, these methods can not characterize directly the strength of reinforced plastics. However, they are helpful in predicting the relationship between the strength of the polymer composite material and the bond strength at the polymer-fiber interface. Proceeding from the general concepts, it can be assumed that under sufficiently high adhesion, a "weak link" in the material would be either a matrix or a fiber. As demonstrated in [5], a correlation between the adhesive strength of the fiber–matrix compound and mechanical properties of reinforced plastics is commonly observed (Fig. 4). The strength of the composite can display a monotonically increasing function of the adhesive strength only within a limited range of values. Under high adhesion, an increase in the bond strength does not cause a proportional increase in the strength of plastic and an overriding trend appears on the curve.

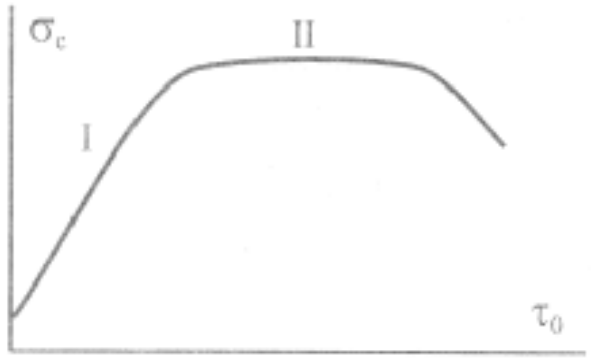

Figure 4. Diagram of the dependence of the composite strength on the adhesive strength of fiber-matrix compounds

Specifics of the dependence - τ_0 is determined by the "weak link" in the composite material, which can be localized by establishing the nature of σ_C — τ_0 dependence.

The above discussed methods and approaches for evaluating the adhesive strength in polymer – fiber systems provide only a conventional value of τ, which largely depends on the scale factor. Assessment of the true adhesive strength is associated with the production of a large number of samples and their testing. This process becomes especially laborious when working with thin (less than 150 μm thickness) fibers.

Another approach to study adhesive interactions involves reinforced plastics under conditions of the emerging shear stresses [6-13]. The strength of composites in the transversal direction (perpendicular to the major fiber orientation) and under interlaminar shear is a measure of adhesive interaction. The shear strength is almost independent of the fiber strength and is determined mainly by the adhesive and cohesive properties of the polymer matrix in a complex stress state.

A three – point bending of relatively short rectangular samples refers to the most common methods for evaluating the shear strength (Fig. 5) [6-9]. The transverse bending of the beam in a three-point pattern creates a complex stress state in the sample and, depending on the ratio between the span length and the sample thickness *l*/h, fracture can occur through bending or interlaminar shear. The value of the maximum tangential shearing stresses calculated by the load at the time moment of the sample fracture by stratification is taken as the shear strength value. In the first approximation, it is calculated by the Zhuravsky formula:

$$\tau_{rq}^{max} = \frac{3}{4} \cdot \frac{P}{b \cdot h} = \tau_{shift} .$$

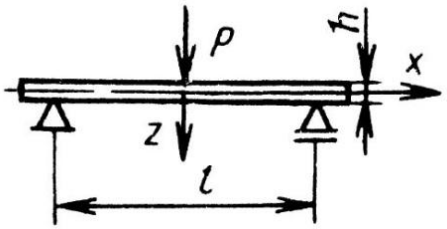

Figure 5. Short-beam bending method, schematic view. a – flat sample, b –convex sample.

Here, formulas for normal stresses in the longitudinal and transversal directions have the following form:

$$\sigma_q^{max} = \frac{3}{2} \cdot \frac{P \cdot 1}{b \cdot h^2} = \sigma_{fl} \; ; \quad \sigma_r^{max} = \frac{3}{8} \cdot \frac{P \cdot 1}{b \cdot h \cdot R} \; ,$$

where P is the fracture load; b, h, R – width, thickness and radius of the ring, respectively.

By equating the load P for tangential and normal stresses, we obtain the value of *l*/ h, when the sample fracture through both mechanisms has equal probabilities:

$$1/\mathrm{h} = \frac{\sigma_{\mathrm{fl}}}{2\tau_{\mathrm{shift}}},$$

i. e., when *l*/h is below this value, the fracture induced by the interlaminar shear prevails, and vice versa (for the bending-induced fracture). The actual fracture from interlaminar shear is observed in the *l*/h range 3-12 and at *l*/ h > 20 – from bending. At *l*/ h < 3, the tested material is destroyed by both bearing and shearing.

This method is characterized by the simplicity of sample manufacturing, which can be either flat or convex, and does not require special fitting. However, the short beam bending method is for reference only and is therefore convenient for comparative tests. It usually produces slightly elevated $\tau_{\text{сдв}}$ values, as compared to other methods. This method is standardized in the Russian Federation (GOST 32659-2014; ISO 14130: 1997; Determination of the apparent tensile strength at interlaminar shear by short beam testing) and internationally (D 2344/D 2344M Standard Test Method for Short-Beam Strength of Polymer Matrix Composite Materials and Their Laminates).

Our study included the following epoxy resins: “ED-22 + IMTHPA”, “Etal Inject-T”, “Etal-245” produced by ZAO ERPC “Epital” (Closed Joint Stock Company); “ARALDITE LY 8615 + XB5173”, HUNTSMAN company production.

The basis for manufacturing flat pressed samples was plain-weave basalt fabric, similar to that of TBK-100, treated with three different experimental lubricants (Fig. 6 (a)).

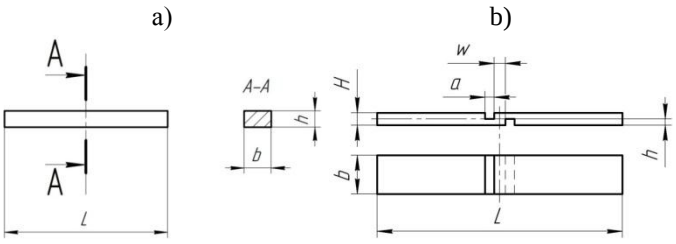

Figure 6. Experimental basalt plastics samples, schematic view: a – flat samples, b - plates with asymmetric notches.

The experimental set of lubricants included “basic”, No. 1 and No. 2, respectively; the following lubricants were used: amino silane–metacryl silane pair: Silane JLSi-1302 Aminofunctionalalkoxysilane – Silane JLSi-3301Methacrylatefunctionalalkoxysilane, PRC production, KV-12M2 and KV-42M2 lubricants produced by “Kamenny vek” LLC.

As noted above, the scale factor plays a significant role in adhesive interaction, i.e., in this case, the shear strength can depend greatly on geometric parameters of *l*/h. In this experiment, the *l*/ h value was changed from 6 to 10 for all sample types. After testing, samples were visually inspected and the type of fracture was identified. Fig. 7 presents the possible types of sample fractures [8]. Only those τ values, which corresponded to the sample fracture induced by tangential shear stress were considered in calculations of the average shear strength.

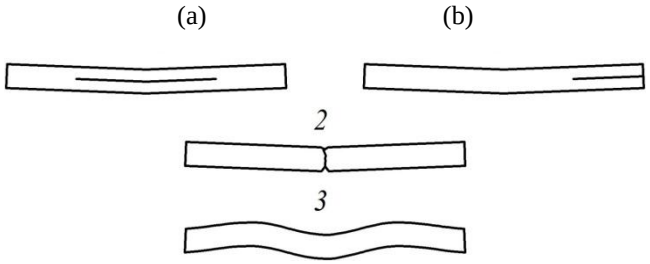

Figure 7. Types of sample fractures under short beam testing. 1 - Fracture from tangential shear stress (a – crack in the middle part of the sample, b – edge crack); 2 – fracture from normal stress (bending); 3 – bearing.

As noted above, the shear strength value derived from the short beam method is slightly higher than that obtained by other test methods. To validate the patterns of shear strength changes in this method, we performed a supplementary survey with the extension method for plates with asymmetric notches.

To assess the effect of the scale factor on the shear strength, notches were applied at a distance of 3-10 mm (Fig. 10 (b)).

Test results

Figs. 8 – 11 demonstrate typical loading diagrams for flat samples of basalt plastics, Figs. 12 – 15 – for samples with asymmetric notches. These loading diagrams allow for the conclusion that in samples tested by the short-beam shear method, loading diagram display several peaks. The first peak corresponds to the basalt plastic strength under shear. Several subsequent load peaks are associated with the residual strength of the material, i.e., several cracks are formed after the first one (breaking) emerged.

Notably, the composition of lubricant has a negligible effect on the loading diagrams profile but the peak levels differ for different lubricant types. For instance, the first peak level was the lowest for the “basic” lubricant, as compared with lubricants No. 1 and 2. The correlation between the secondary peak levels in fractured samples treated with different lubricants is generally similar to those of the primary peak levels.

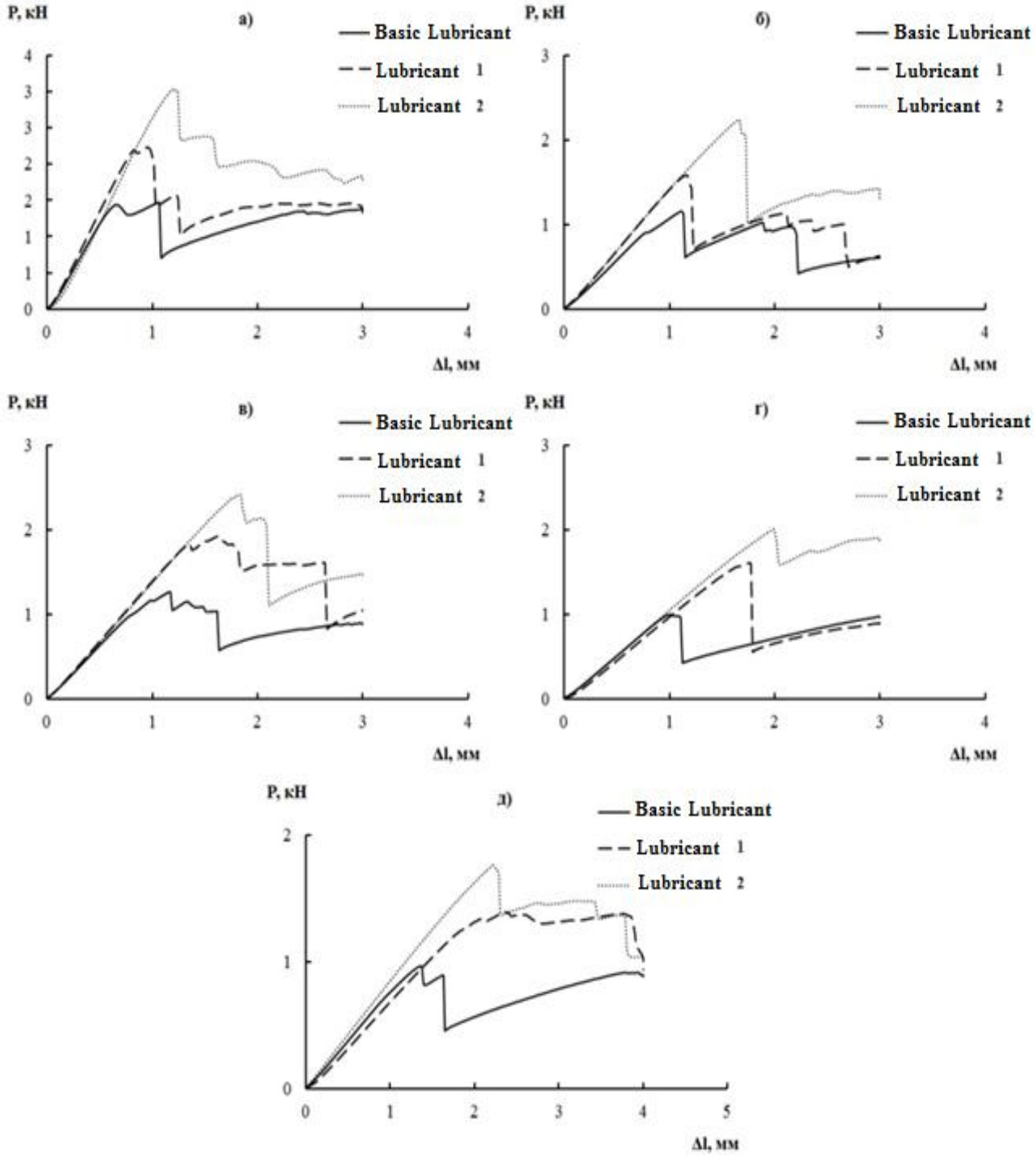

Figure 8. Typical loading diagrams for flat samples of basalt plastics based on ARALDITE LY8615 cold-setting epoxy resin: а – *l*/h = 6; б – *l*/h =7; в – *l*/h = 8; г – *l*/h = 9; д – *l*/h = 10. The lubricant type is indicated in the diagram.

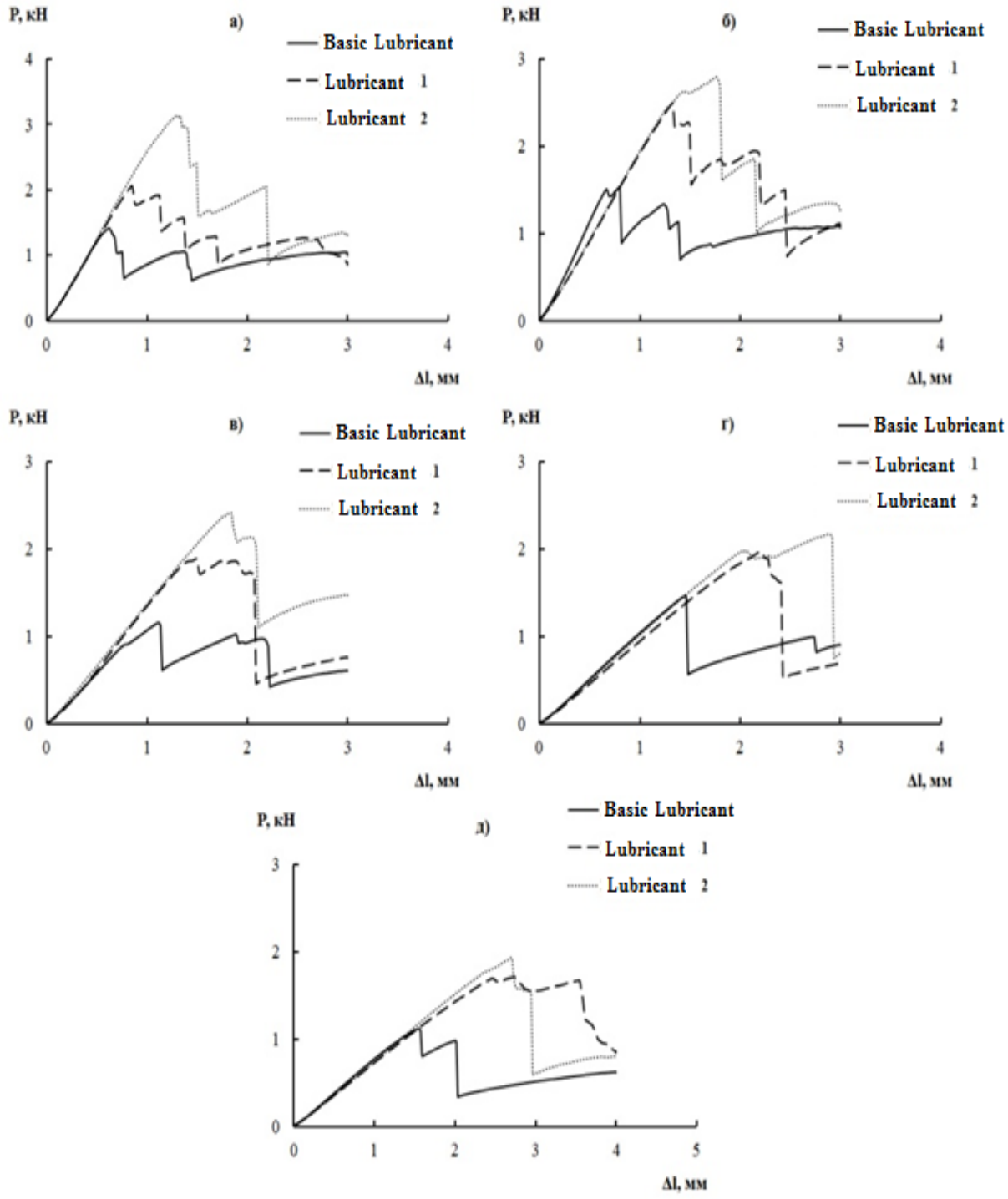

Figure 9. Typical loading diagrams for flat samples of basalt plastics based on ED-22 epoxy resin and iso- IMTHPA hardener: а – *l*/h = 6; б – *l*/h =7; в – *l*/h = 8; г – *l*/h = 9; д – *l*/h = 10. The lubricant type is indicated in the diagram.

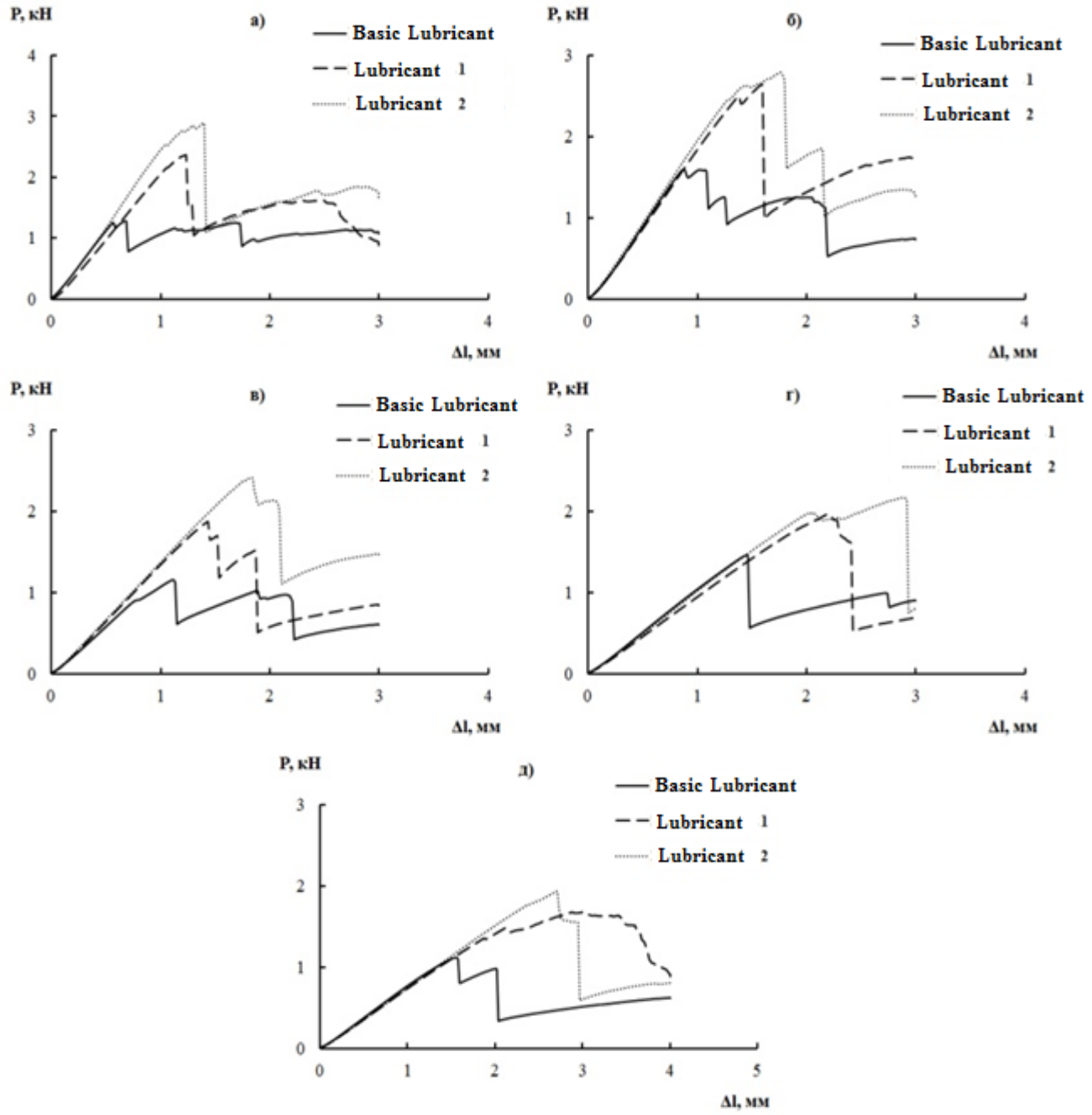

Figure 10. Typical loading diagrams for flat samples of basalt plastics based on Etal-245 epoxy resin: а – *l*/h = 6; б – *l*/h =7; в – *l*/h = 8; г – *l*/h = 9; д – *l*/h = 10. The lubricant type is indicated in the diagram.

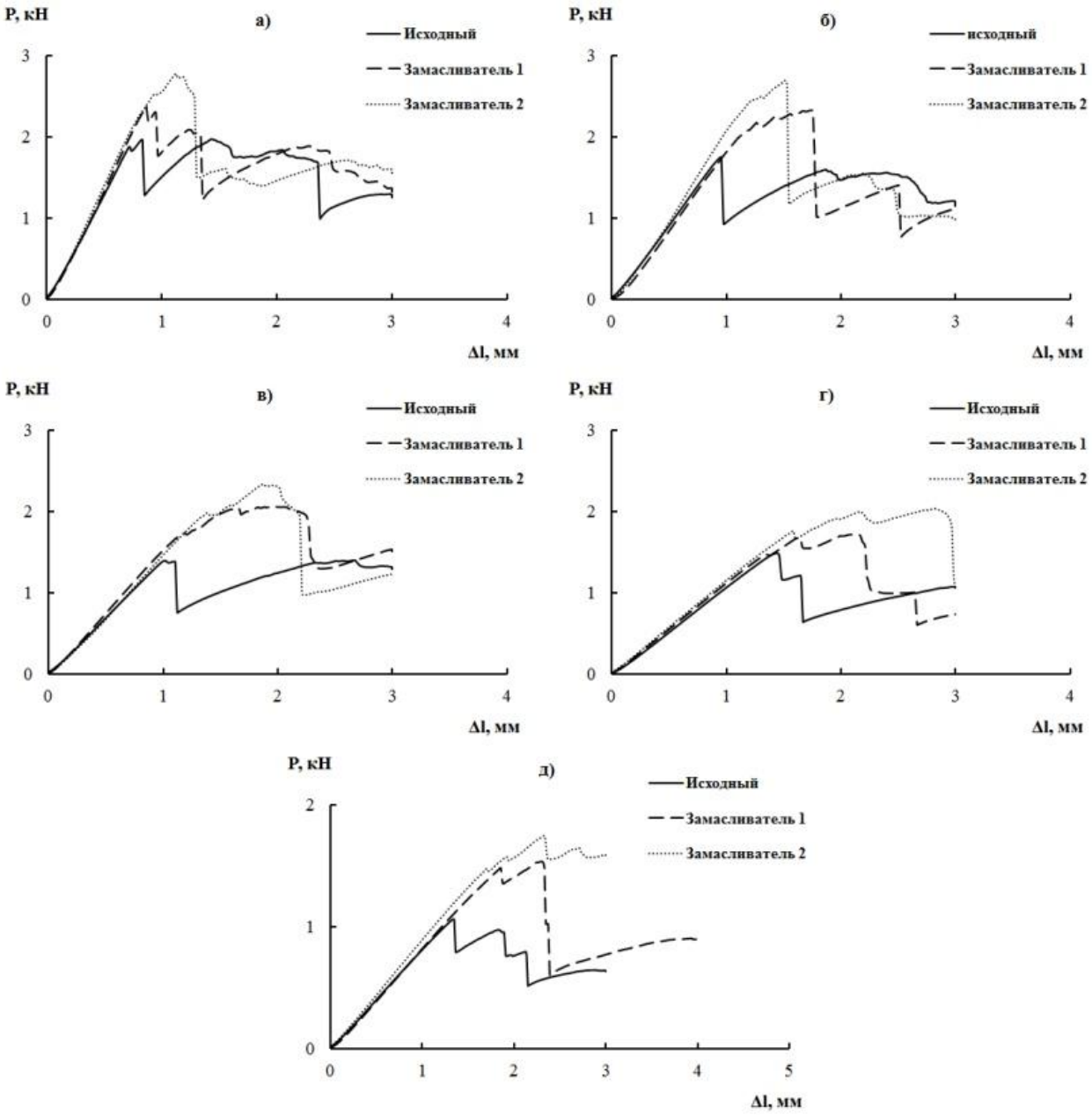

Figure 11. Typical loading diagrams for flat samples of basalt plastics based on Etal-Inject T epoxy resin: а – *l*/h = 6; б – *l*/h =7; в – *l*/h = 8; г – *l*/h = 9; д – *l*/h = 10. The lubricant type is indicated in the diagram.

Similarly, the type of binder has little effect on the appearance of loading diagrams and the height of primary and secondary peaks. The type of hardeners and, accordingly, curing modes are also insignificant, as well as changes in the l/h ratio. An increase in the *l*/ h value leads to the decrease in loads taken by the material. The type of lubricant or the binder does not affect this trend, too.

Unlike the case with the short-beam shear, samples with asymmetric notches are destroyed when the load corresponding to their strength is reached (Figs. 12 – 15). Probably, this fracture mechanism happens because the crack spreads between the layers of reinforcing filler almost instantly when the critical stress is reached. The same as for the short-beam shear, the maximum load level is determined by the type of lubricant, which was used to treat the reinforcing filler. In the case of "basic" lubricant, the maximum load is lower than for lubricants No. 1 and 2. This trend persists for both epoxy and polyester binders. Also, the type of epoxy hardener has no great effect on the appearance of load diagrams, as well as changing the distance between notches. Such independence is typical for various types of binders and hardeners, as well as for all lubricants used for treating basalt fibers.

Thus, we can tentatively conclude that the studied lubricants, types of binders, hardeners and thermal treatment modes practically do not affect the profiles of loading diagrams, and,

consequently, the fracture mechanisms in basalt plastics. It should be noted that all studied samples were destroyed through tangential shear stresses, as identified visually after the fracture of each sample.

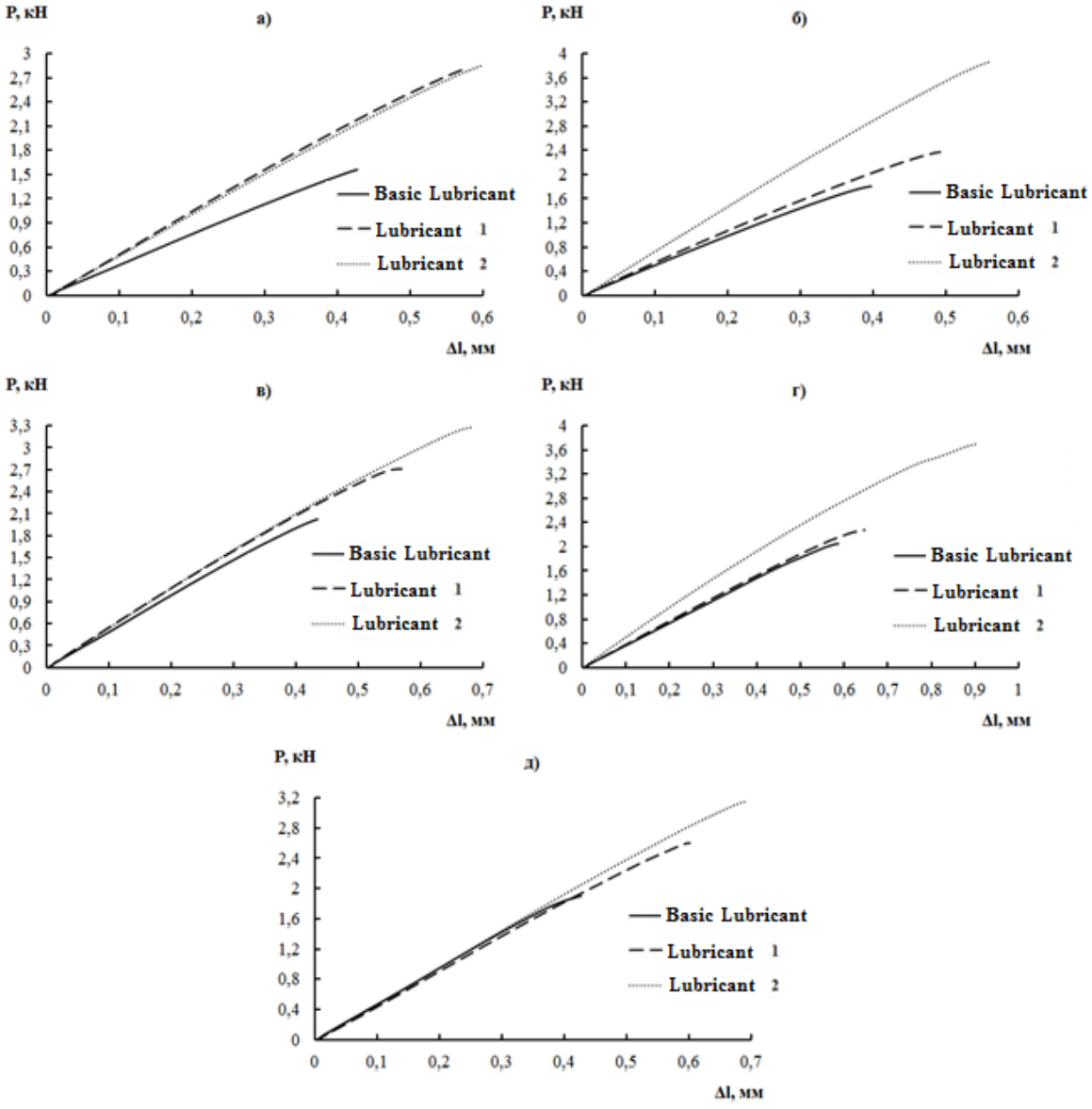

Figure 12. Typical loading diagrams for samples with asymmetric notches of basalt plastics based on ARALDITE LY8615 cold-setting epoxy resin. The distance between notches: а – 3; б – 5; в – 6.5; г – 8; д – 10. The lubricant type is indicated in the diagram.

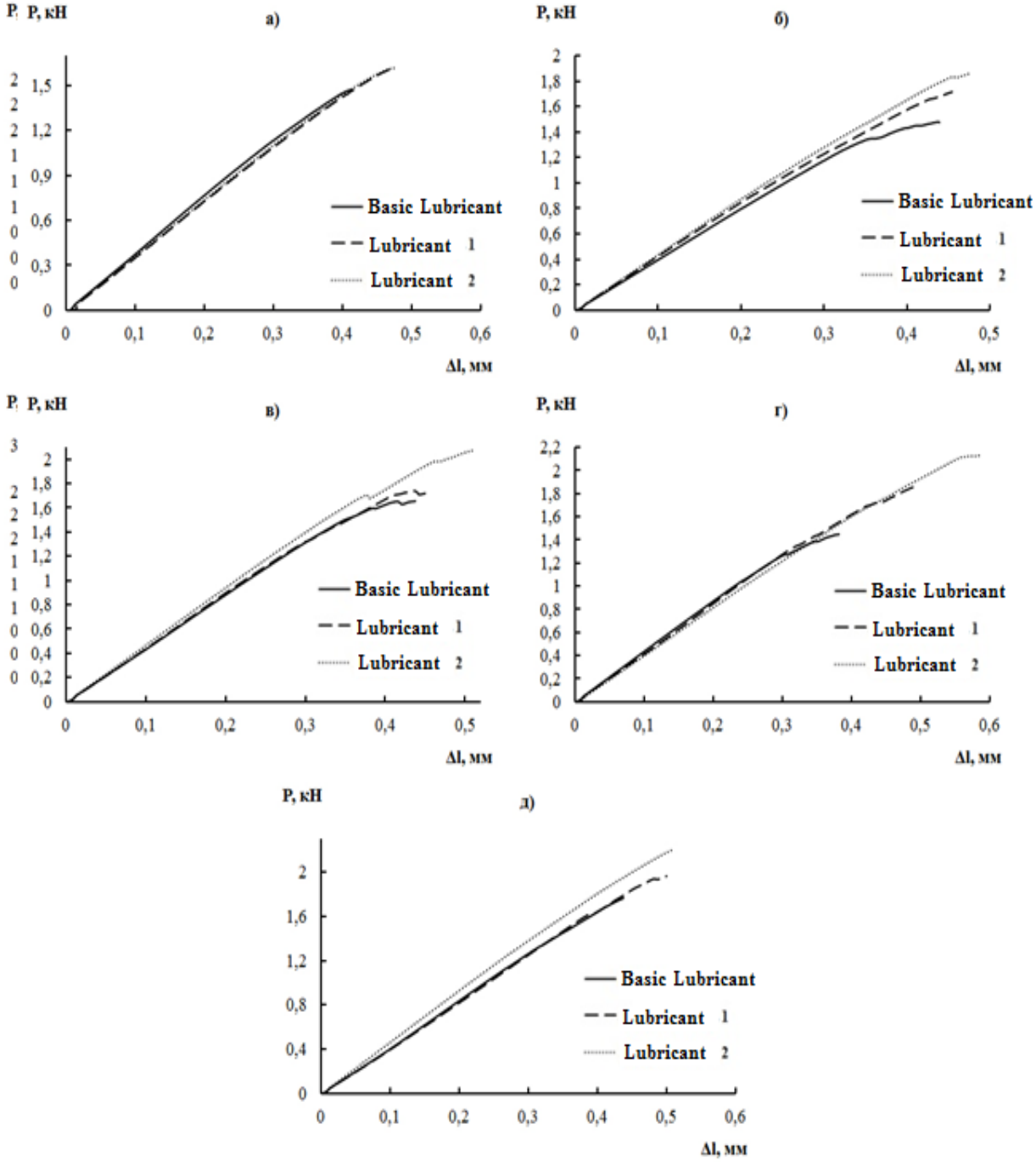

Figure 13. Typical loading diagrams for samples with asymmetric notches of basalt plastics based on ED-22 epoxy resin and iso-IMTHPA hardener. The distance between notches: а – 3; б – 5; в – 6.5; г – 8; д – 10. The lubricant type is indicated in the diagram.

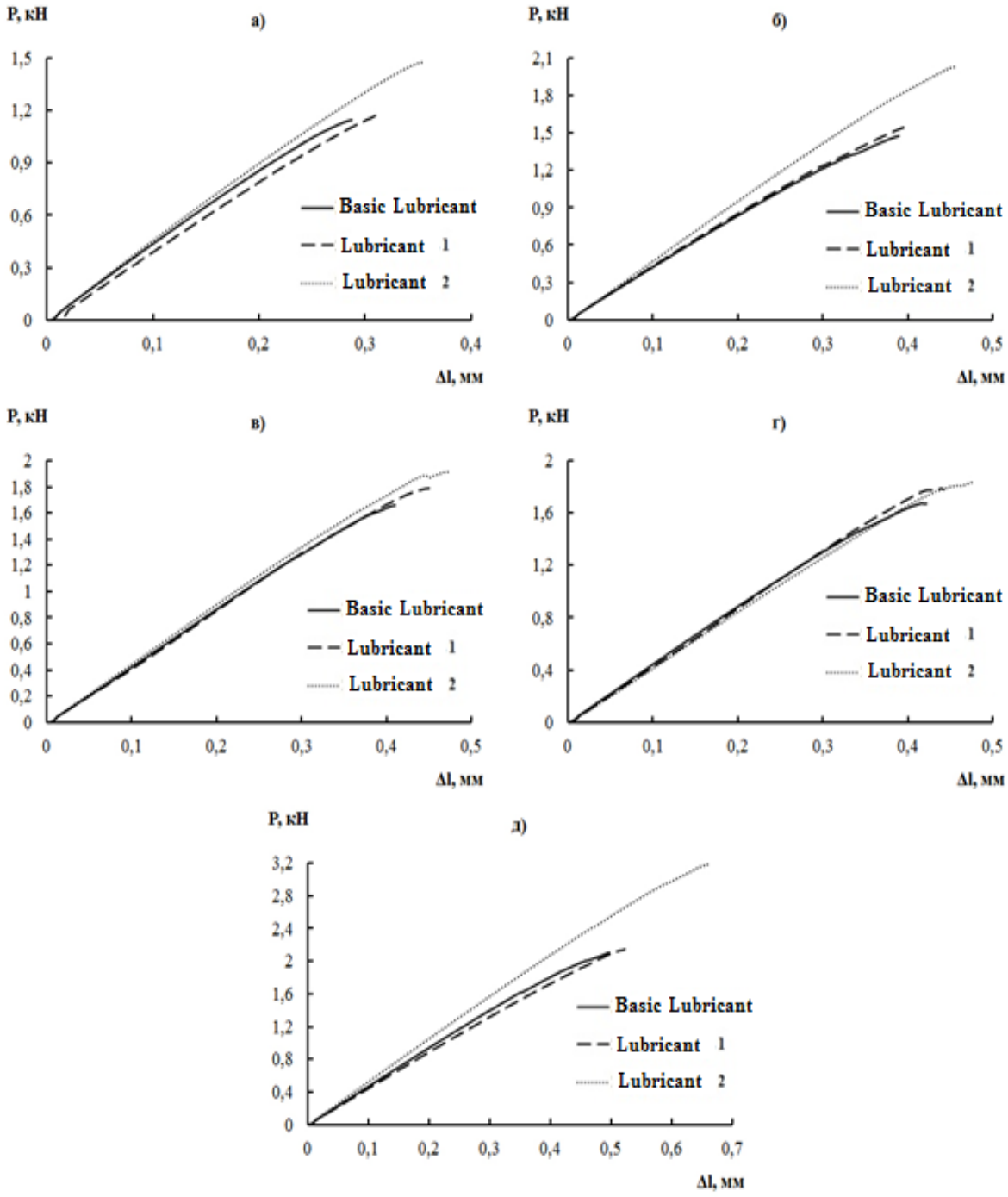

Figure 14. Typical loading diagrams for samples with asymmetric notches of basalt plastics based on Etal-245 epoxy resin. The distance between notches: а – 3; б – 5; в – 6.5; г – 8; д – 10. The lubricant type is indicated in the diagram.

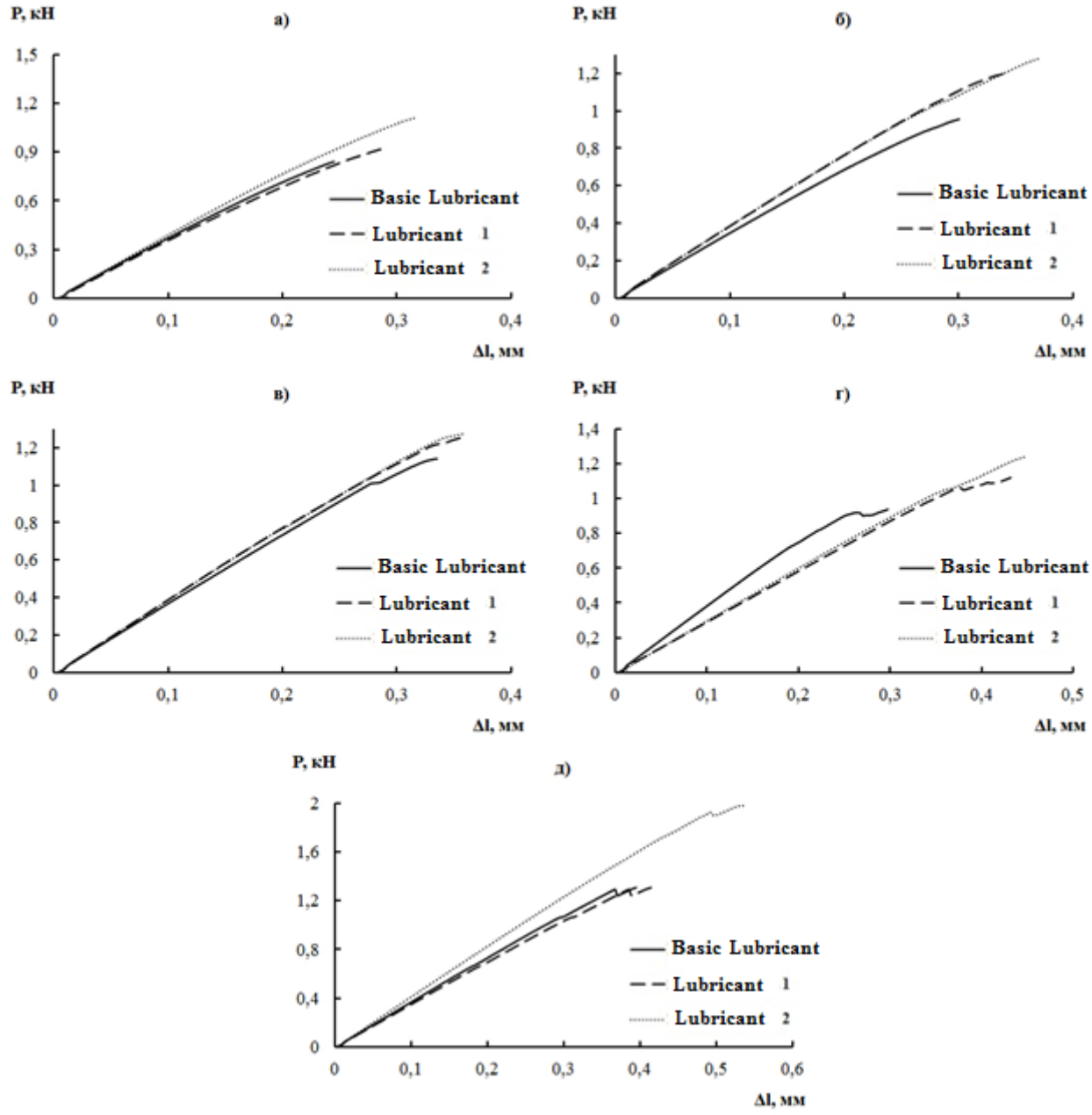

Figure 15. Typical loading diagrams for samples with asymmetric notches of basalt plastics based on Etal-Inject T epoxy resin. The distance between notches: а – 3; б – 5; в – 6.5; г – 8; д – 10. The lubricant type is indicated in the diagram.

The pattern of the effect of lubricants and geometric factor on the basalt plastics strength under shear is clearly demonstrated in Figs. 16 – 19. Flat samples made of a fabric treated with various types of lubricants and tested by the short-beam shear method (Fig. 16) are characterized by a decrease in shear strength against the increase in *l*/h ratio. The decline in shear strength is observed for all types of lubricants and all studied matrices. In this case, the τ value decreases by 40 %, on average, as compared with the strength at *l*/ h = 6. A steeper pattern of the τ – *l*/h dependences is observed for basalt plastics based on "Etal-Inject T2" and "PN-609-21M" binders. Probably, such drastic decline in the shear strength against increasing *l*/ h is associated with the higher residual stresses emerging at the polymer–fiber interface, in the first case – due to the high (150 °C) curing temperature, and in the second – due to the high curing rate of the polyester binder. In both cases, the decrease in shear strength slightly exceeds 50 %. Fig. 16 also demonstrates clearly that the shear strength has its own specific level for each lubricant. For example, the τ – *l*/h dependence is placed lower for the basic lubricant than for No. 1 and 2, respectively. The difference in the strength between the base and No. 1 lubricants is about 20 %, on average, and up to 40 % in the case of the basic and No. 2 lubricants.

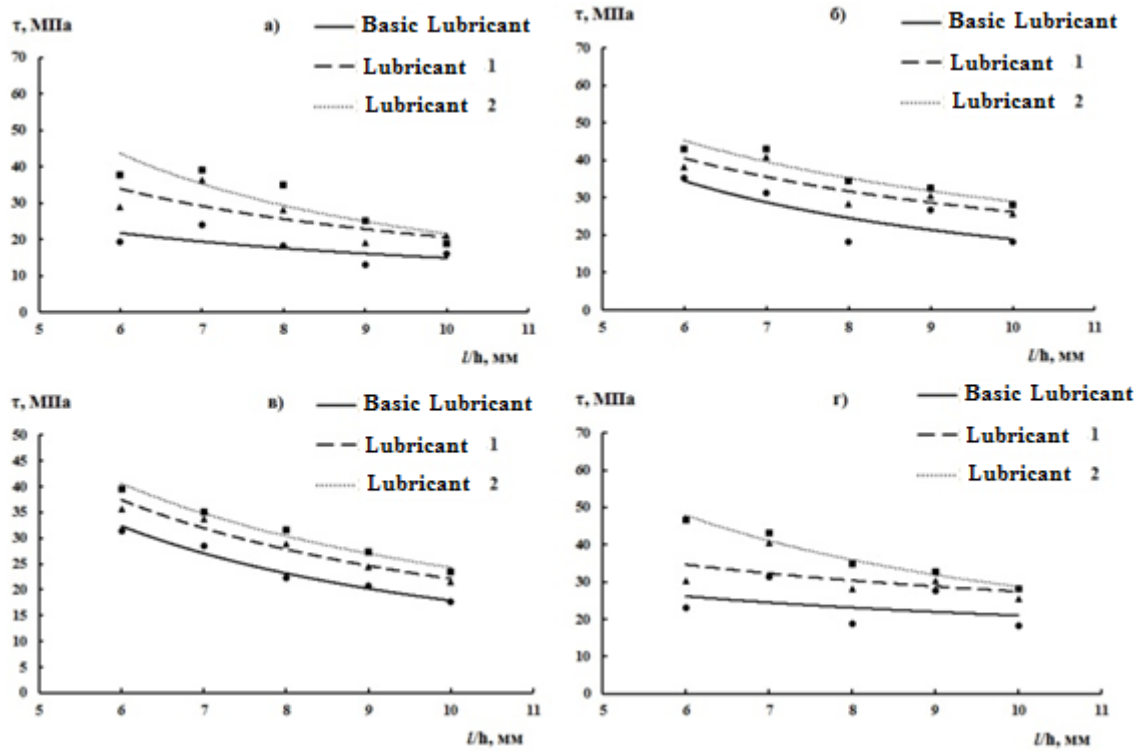

Figure 16. Dependence of the shear strength τ from the *l*/h value, flat basalt plastic samples based on a fabric treated with various lubricants: а – ARALDITE LY8615; б – Etal-245; в – Etal-Inject T; г – ED-22 + iso-IMTHPA; д – PN-609-21M. The lubricant type is indicated in the diagram.

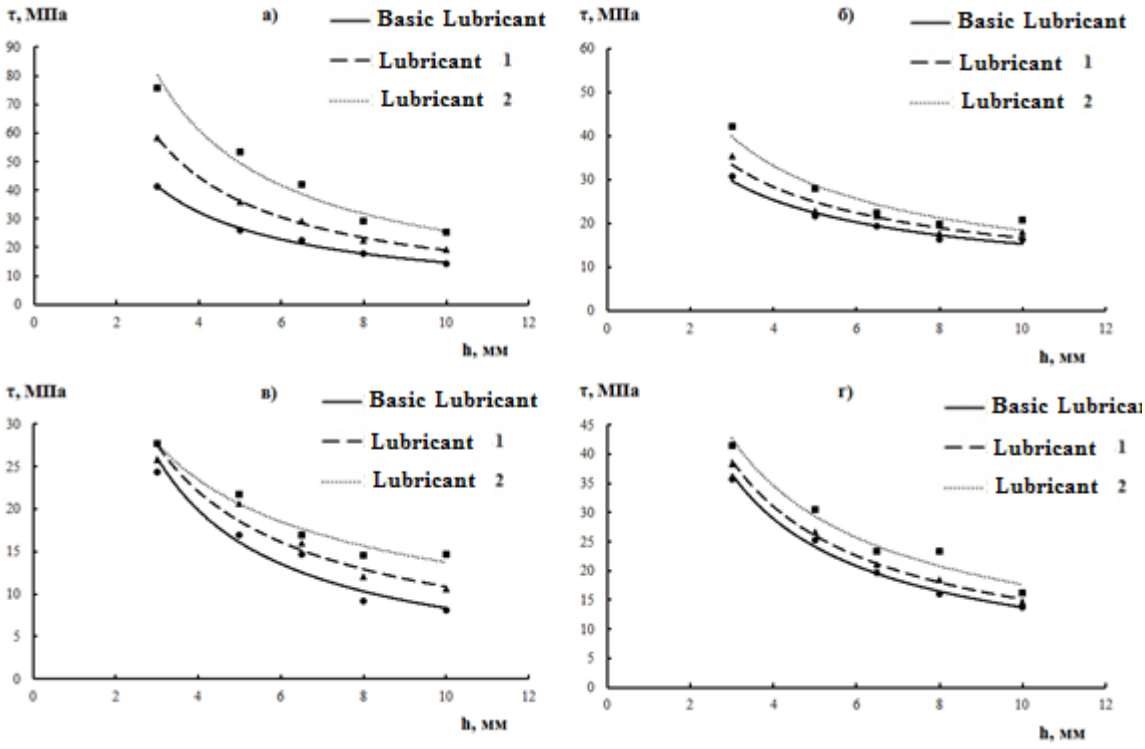

Figure 17. Dependence of the shear strength τ from the distance between notches in basalt plastic samples based on a fabric treated with various lubricants: а – ARALDITE LY8615; б – Etal-245; в – Etal-Inject T; г – ED-22 + iso-IMTHPA. The lubricant type is indicated in the diagram.

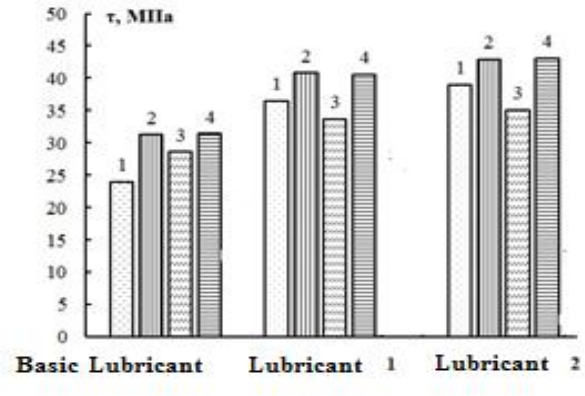

Figure 18. Shear strength in pressed basalt plastics based on a fabric treated with different types of lubricants and thermosetting binders: 1 – ARALDITE LY8615; 2 – Etal-245; 3 – Etal-Inject T; 4 – ED-22 + iso-IMTHPA.

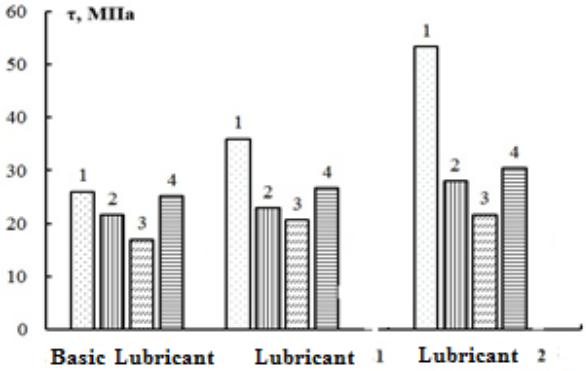

Figure 19. Shear strength in samples with asymmetric notches of basalt plastics based on a fabric treated with different types of lubricants and thermosetting binders: 1 – ARALDITE LY8615; 2 – Etal-245; 3 – Etal-Inject T; 4 – ED-22 + iso-IMTHPA. The distance between notches is 6.5 mm.

Table 1. Comparison of the shear strength in basalt plastics, test methods and modes of their formation.

Curing temperature, °C		25	110	110	150
Molding temperature, °C		25	70	70	70
Test method, type of samples	Matrix composition / Type of lubricant	ARALDITE LY8615+ XB 5173 HARDENER	ЭД-22+ и-МТГФА	Etal-245	Etal-Inject T
Short beam method, flat samples (l / h = 7)	Basic	24.0	31.4	31.3	28.6
	Lubricant No. 1	36.5	40.6	40.8	33.7
	Lubricant No. 2	39.0	43.1	42.9	35.1
Evaluation of shear strength, flat samples with asymmetric notches (w = 6.5)	Basic	22.5	19.7	19.4	14.7
	Lubricant No. 1	29.1	21.1	21.7	16.0
	Lubricant No. 1	42.1	23.4	22.5	17.0

CONCLUSION

In this study, we used multiple practical approaches to estimate the shear strength components and the degree of manifestation of adhesion factor in strength tests of the experimental epoxy basalt plastic samples.

The values of shear strength obtained in the experimental conditions ranged within 21.2-51.3 MPa (see Table 1), depending on the "binder – lubricant" combination.

These data reflect confidently the shear strength dependence on the quality of the epoxy binder. The range of shear strength increment makes up to 30-35% under a combination of the same lubricant and various binders.

The importance of the correctly selected lubricant, which determines adhesion affinity between the fiber and the matrix is clearly demonstrated by the range of shear strength variation defined experimentally, up to 100 % increase, depending on the type of lubricant and in combination with the same binder.

These findings provide a wide field for the practical technological formulations, with view of manufacturing basalt plastic products with enhanced strength characteristics.

REFERENCES

[1] Gorbatkina Yu.A. Adhesive strength in polymer-fiber systems. – M.: Chemistry, 1987. - 192 p.

[2] Estenburg R.B. Phoenix S.L. Interfacial shear strength studies using the single-filament-composite test/ Pt. II: A probability model and Monte Carlo simulation // Polymer composites. – 1989. – Vol.10, No 5. – p. 389-408.

[3] Ulkem I., Shreiber H.P. The role of interactions at interfaces of glass-fiber reinforced composites // Composite Intefaces.-1994. – Vol. 2, No 4. – p. 253-256

[4] G.S. Shul, Yu.A. Gorbatkina, G.P. Mashinskaya. Effect of chemical nature of matrix on the strength of bonds with Armos aramide fibers // Mechanics of composite materials. - 1998. - Vol. 34, No 3. – p. 391-406.

[5] Gorbatkina, Yu.A. Correlation between the strength of fiber-reinforced plastics and the adhesive strength of fiber - matrix joints // Mechanics of composite materials. - 2000. - Vol. 36. - No 3. - p. 291.

[6] Composite materials / V.V. Vasilyev, Yu.M. Tarnapolsky (Eds.). M .: Industrial Engineering, 1990. 512 pp.

[7] Reinforced plastics / G.S. Golovkin, V.I. Semenov (Eds.). M.: MAI Publishers, 1997. 404 pp.

[8] Composite materials / L. Brautman (Ed.), G.P. Cherepanov (English translation). Vol. 5, M.: Mir, 1978. 484 pp.

[9] Tarnapolsky Yu.M., Kinis T.Ya. Methods of static testing of reinforced plastics. M.: Chemistry, 1975, 264 pp.

[10] Capillary hydrodynamics of oligomer binders. Nelyub, V.A., Borodulin, A.S., Kobets, L.P., Malysheva, G.V. 2016 Polymer Science - Series D 9(3), p. 322-325

[11] Nelyub, V.A. Determination of adhesive interaction between carbon fiber and epoxy binder. 2015. Polymer Science - Series D, 8(1), p. 6-8.

[12] Nelyub, V.A., Borodulin, A.S., Kobets, L.P., Malysheva, G.V. A study of structure formation in a binder depending on the surface microrelief of carbon fiber. 2016 Polymer Science - Series D

[13] Nelyub, V.A. Method for Assessing the Chemical Reaction Between Carbon Fibre and Epoxide Binder. 2015 Fibre Chemistry 47(1), p. 40-42.